Open Research Online

The Open University's repository of research publications
and other research outputs

Special quasirandom structures for gadolinia-doped ceria and related materials

Journal Item

How to cite:

Wang, H.; Chroneos, Alexander; Jiang, C. and Schwingenschlögl, U. (2012). Special quasirandom structures for gadolinia-doped ceria and related materials. Physical Chemistry Chemical Physics, 14(33) pp. 11737–11742.

For guidance on citations see FAQs.

© 2012 Royal Society Chemistry

Version: Version of Record

Link(s) to article on publisher's website:
http://dx.doi.org/doi:10.1039/c2cp41202k

Copyright and Moral Rights for the articles on this site are retained by the individual authors and/or other copyright owners. For more information on Open Research Online's data policy on reuse of materials please consult the policies page.

oro.open.ac.uk

View Online / Journal Homepage / Table of Contents for this issue
Dynamic Article Links

PCCP

Cite this: *Phys. Chem. Chem. Phys.*, 2012, **14**, 11737–11742

www.rsc.org/pccp

PAPER

Special quasirandom structures for gadolinia-doped ceria and related materials

H. Wang,[a] A. Chroneos,*[b] C. Jiang[c] and U. Schwingenschlögl*[a]

Received 14th April 2012, Accepted 6th July 2012
DOI: 10.1039/c2cp41202k

Published on 09 July 2012 on http://pubs.rsc.org | doi:10.1039/C2CP41202K
Downloaded by Open University on 20 October 2012

Gadolinia doped ceria in its doped or strained form is considered to be an electrolyte for solid oxide fuel cell applications. The simulation of the defect processes in these materials is complicated by the random distribution of the constituent atoms. We propose the use of the special quasirandom structure (SQS) approach as a computationally efficient way to describe the random nature of the local cation environment and the distribution of the oxygen vacancies. We have generated two 96-atom SQS cells describing 9% and 12% gadolinia doped ceria. These SQS cells are transferable and can be used to model related materials such as yttria stabilized zirconia. To demonstrate the applicability of the method we use density functional theory to investigate the influence of the local environment around a Y dopant in Y-codoped gadolinia doped ceria. It is energetically favourable if Y is not close to Gd or an oxygen vacancy. Moreover, Y–O bonds are found to be weaker than Gd–O bonds so that the conductivity of O ions is improved.

Introduction

A criterion for solid oxide fuel cells (SOFCs) to become economical is the operation in the intermediate temperature range (500–700 °C).[1] However, this temperature range presents difficulties for the operation of traditional ceramic cathodes and electrolytes and requires materials with enhanced O diffusion.[2] Numerous candidate oxides are being investigated for cathode and electrolyte applications for the next generation of intermediate temperature SOFCs (IT-SOFCs).[3–8] The research community is looking for alternative ways to enhance the ionic transport, such as the formation of an interface between dissimilar oxides.[9–15] For example, Barriocanal *et al.*[13] have determined that in strained interfaces between $SrTiO_3$ and yttria stabilized zirconia (YSZ) the ionic conductivity can be increased by eight orders of magnitude. Recent calculations using density functional theory (DFT) support the enhancement in ionic conductivity in YSZ/$SrTiO_3$ interfaces but point towards a more moderate increase (up by about 3.5 orders of magnitude).[15] More conventional methods for enhancing the conductivity of YSZ involve codoping. For example, Xie *et al.*[16] have observed an increase in YSZ co-doped with gadolinia in both experiments and molecular dynamics calculations.

The aggressive strain and extensive doping regimes require an understanding of the fundamental defect processes of materials such as YSZ and gadolinia doped ceria (GDC) that need to be effectively reinvented to be considered in the next generation of IT-SOFCs. The understanding of these materials is complicated by the random distribution of the cation and oxygen vacancies on the lattice sites. The present study aims to contribute towards the understanding of the effect of the local cation environment and oxygen vacancy distribution on the defect processes of GDC and related materials. We have generated two 96-atom special quasirandom structure (SQS) cells describing 9% and 12% gadolinia in GDC compositions which are technologically important. As an example, we use DFT calculations to study the effect of the local environment around a Y dopant in Y-codoped GDC and discuss the results in view of theory and experiments.

Methodology

A. Special quasirandom structure generation

DFT methods often rely on the construction of supercells with periodic boundary conditions. The calculations are straightforward for ordered systems. However, for systems which display atomic disorder they can be more complicated. Using a brute force approach the disordered system can be described by constructing a large supercell and randomly inserting the cations (here Gd or Ce) on their sublattice. In practical terms this is not feasible for DFT calculations as large supercells are required to adequately reproduce the statistics of random alloys.

With the SQS approach it is possible to adequately mimic the statistics of a random alloy in a relatively small supercell.[17–21] In essence, SQSs are specially designed small-unit-cell periodic structures that closely mimic the most relevant near neighbor

[a] *PSE Division, KAUST, Thuwal 23955-6900, Saudi Arabia. E-mail: udo.schwingenschlogl@kaust.edu.sa; Tel: +966 544700080*
[b] *Department of Materials, Imperial College London, London SW7 2BP, UK. E-mail: alexander.chroneos@imperial.ac.uk*
[c] *State Key Laboratory of Powder Metallurgy, Central South University, Changsha, Hunan 410083, China*

Published on 09 July 2012 on http://pubs.rsc.org | doi:10.1039/C2CP41202K
Downloaded by Open University on 20 October 2012

pair and multisite correlation functions of random substitutional alloys. Due to the atomistic nature of the SQS approach, a distribution of distinct local environments existing in real random alloys is maintained, which is essential for the present work.

B. DFT calculations

The Vienna *Ab initio* Simulation Package (VASP)[22] is used to investigate how Y doping affects the oxygen vacancy diffusion in $Ce_{26}Gd_6O_{61}$. The exchange correlation is treated in the generalized gradient approximation of the Perdew–Burke–Ernzerhof edition.[23] Pseudopotentials generated by the projector augmented wave method[24] are employed. Convergence is achieved with a Gamma-centred 3 × 3 × 3 k-mesh. Kr $4d^{10}$ and Xe are considered to be the core states of Ce and Gd, respectively. The experimental lattice constant of 5.423 Å for $Ce_{0.8}Gd_{0.2}O_{1.9}$[25] is used in our calculations of the $Ce_{26}Gd_6O_{61}$ SQS supercell.

The on-site coulomb interaction[26] is taken into account for the localized Ce 4f and Gd 4f orbitals. There are many choices for U parameters of Ce 4f in different situations, so that a test is necessary for our specific case. The experiment shows that Gd-doped CeO_2 is ferromagnetic at 5 K.[27] Thus, not spin polarized and spin polarized calculations are performed for the (U, J) candidates (5, 0),[28,29] (6.1, 0),[30] (6.7, 0.7),[31] and (7, 0).[32] Furthermore, the lattice constants and atomic positions are optimized with an energy cut-off of 520 eV to find out the effects of different U and J parameters.

Results and discussion

A. SQS structure

In essence Gd and Ce atoms can randomly occupy equivalent lattice sites in GDC. Consequently, the formation of oxygen vacancies will occur with a multitude of distinct local arrangements of the surrounding host cations. These arrangements will affect the formation and migration of the oxygen vacancies. The representation of the random alloy by a very large supercell and the random occupation of the cation sublattice with Gd and Ce atoms to mimic the random nature of GDC is a computationally intractable approach to study defect processes using DFT.

As the fcc cation and simple-cubic anion sublattices do not exchange species, the configurational problem can be greatly simplified to that of a binary system. Thus, the total energy of the system depends on two types of interatomic interactions: those between atoms on the same sublattice (cation–cation and anion–anion) and those between atoms on different sublattices (cation–anion). We have generated two 96-atom SQSs corresponding to the compositions $Ce_{26}Gd_6O_{61}$ (or 9% gadolinia doped GDC) and $Ce_{24}Gd_8O_{60}$ (or 12% gadolinia doped GDC).[20] Table 1 gives the pair correlation functions of the generated SQSs in comparison with those of the random alloy. It can be observed that both the nearest-neighbor intrasublattice and intersublattice pair correlation functions of the random GDC structure are accurately reproduced by the SQS. The SQSs are presented in Fig. 1 in their ideal, unrelaxed forms. In Fig. 2 we show the atomic shifts during the relaxation of $Ce_{26}Gd_6O_{61}$ by black arrows. As expected, the largest shifts appear in the vicinity of the vacancies.

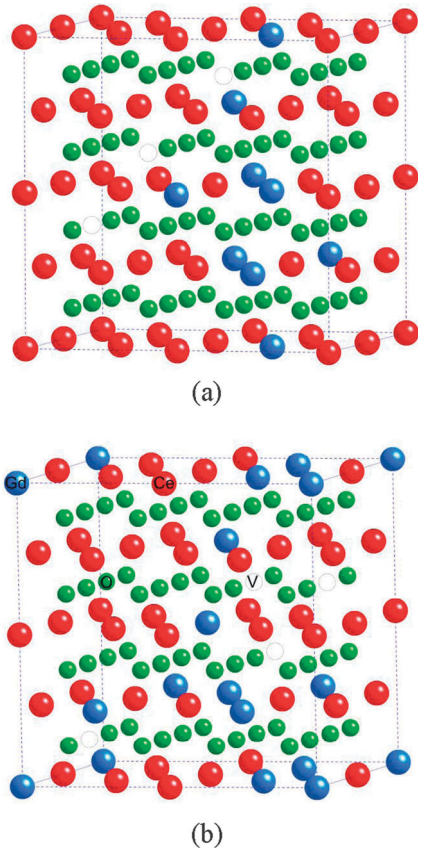

Fig. 1 96-atom SQS corresponding to compositions (a) $Ce_{26}Gd_6O_{61}$ (or 9% gadolinia doped GDC) and (b) $Ce_{24}Gd_8O_{60}$ (or 12% gadolinia doped GDC). Red (large light gray) spheres represent the Ce ions, blue (large dark gray) spheres the Gd ions, green (small) spheres the O ions and dotted circles the O vacancies.

B. $Ce_{26}Gd_6O_{61}$

For comparison, we address in Fig. 3 the electronic structure of CeO_2. The valence band is dominated by the O 2p states

Table 1 Intrasublattice (cation–cation and anion–anion) and intersublattice (cation–anion) pair correlation functions of the 96-atom SQS structures that mimic random GDC compounds (nn = nearest neighbor)

		Cation–cation			Anion–anion				Cation–anion		
Composition	Structure	1 nn	2 nn	3 nn	1 nn	2 nn	3 nn[a]	3 nn[a]	1 nn	2 nn	3 nn
$Ce_{26}Gd_6O_{61}$	Random	0.391	0.391	0.391	0.821	0.821	0.821	0.821	0.566	0.566	0.566
	SQS-96	0.396	0.417	0.375	0.813	0.823	0.844	0.813	0.563	0.568	0.573
$Ce_{24}Gd_8O_{60}$	Random	0.25	0.25	0.25	0.766	0.766	0.766	0.766	0.438	0.438	0.438
	SQS-96	0.25	0.25	0.25	0.771	0.760	0.781	0.750	0.438	0.438	0.438

[a] For anion–anion interaction, two distinct 3 nn pairs exist depending on whether a cation sits in between the two anions.

 This journal is © the Owner Societies 2012

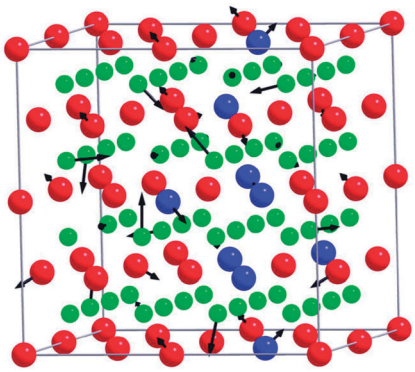

Fig. 2 Atomic shifts during the force minimization of the $Ce_{26}Gd_6O_{61}$ SQS cell. The lengths of the black arrows are proportional to the shifts of the atoms, where only shifts larger than 0.06 Å are indicated. The largest observed shift amounts to 0.28 Å.

with considerable contributions of the Ce 4f states due to finite hybridization. In addition, the Ce 4f states give rise to a pronounced peak around 2.5 eV. Spin polarized calculations with different U and J parameter sets produce for $Ce_{26}Gd_6O_{61}$ almost the same lattice parameters, band gap, and total energy as the not spin polarized one. The total DOS of the not spin polarized and spin polarized calculations with $U_{4f} = 5$ eV and $J_{4f} = 0$ eV for Ce is shown in Fig. 4. Neither spin splitting in the total DOS nor a magnetic moment is obtained. The experiment indicates that the remanent magnetization is very weak (in the order of 10^{-3} emu), where the ferromagnetism arises from the Ce^{3+} and Gd^{3+} ions.[27,33] However, the ferromagnetic ground state is not reproduced in the simulation because of the shortcomings of the ideal structure. Finally, we retain the spin polarized setting for all calculations to be consistent with the experimental determinations of ferromagnetism.

Comparing the results of different (U, J) sets for the Ce 4f orbitals, the lattice constants increase and are larger than the experimental value.[25] The band gaps are smaller than the experimental value of Gd-doped CeO_2 (Ce : Gd = 9 : 1), which is well known for DFT calculations. As the band gap almost does not vary for different Ce U_{4f} and J_{4f} parameters,

Downloaded by Open University on 20 October 2012
Published on 09 July 2012 on http://pubs.rsc.org | doi:10.1039/C2CP41202K

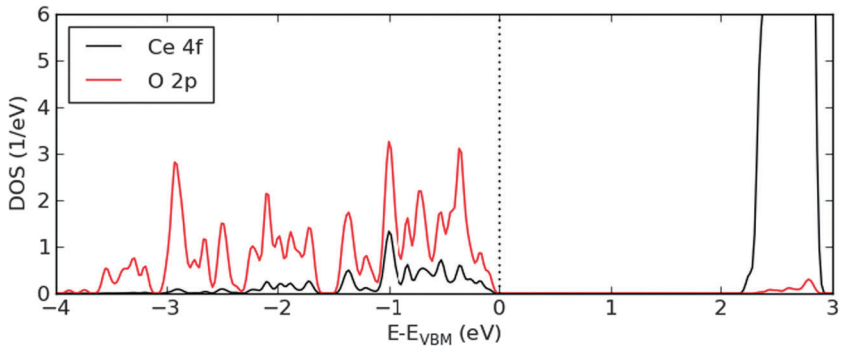

Fig. 3 PDOS of Ce 4f and O 2p in CeO_2.

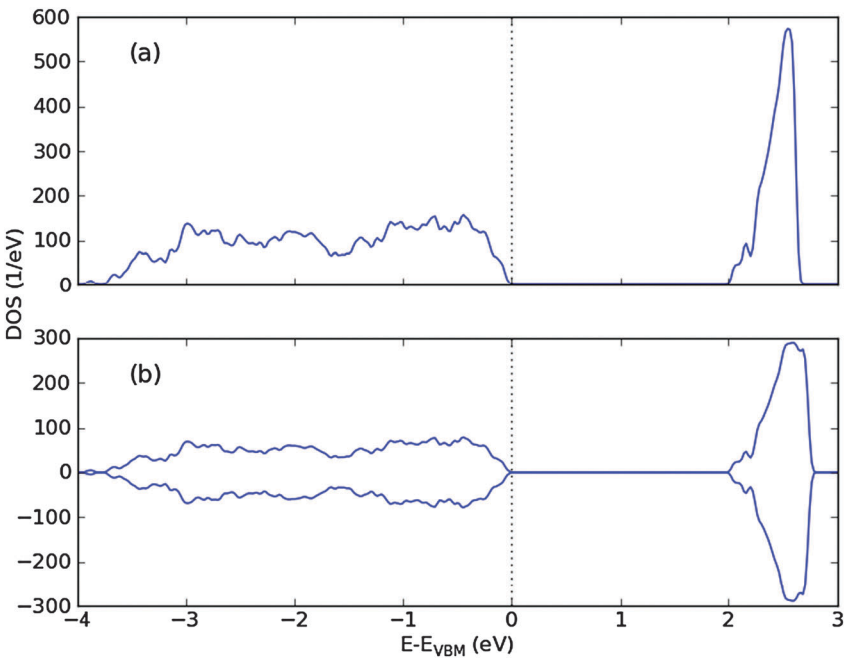

Fig. 4 Total DOS of $Ce_{26}Gd_6O_{61}$ for non-spin polarized (a) and spin polarized (b) calculations with Ce $U_{4f} = 5$ eV, $J_{4f} = 0$ eV and Gd $U_{4f} = 6.7$ eV, $J_{4f} = 0.7$ eV.

Published on 09 July 2012 on http://pubs.rsc.org | doi:10.1039/C2CP41202K
Downloaded by Open University on 20 October 2012

Table 2 Crystal structure parameters and band gap of $Ce_{26}Gd_6O_{61}$ after full relaxation with spin polarized calculations and Ce U_{4f} = 5 eV, J_{4f} = 0 eV, and Gd U_{4f} = 6.7 eV, J_{4f} = 0.7 eV comparing with experiment

	DFT calculation	Experiment
a (Å)	5.547	5.426[a]
b (Å)	5.548	
c (Å)	5.553	
Angle	89.4 90.0 89.9	90[a]
Band gap (eV)	2.0	2.48[b]

[a] Lattice parameters for $Ce_{0.8}Gd_{0.2}O_{1.9}$.[25] [b] Band gap of Gd-doped CeO_2 (Gd : Ce = 1 : 9).[27]

we choose U_{4f} = 5 eV and J_{4f} = 0 eV to obtain lattice constants which are closest to the experimental values. This parameter set has been widely used for CeO_2.[28,29]

The effect of U and J for Gd 4f orbitals is also investigated in spin polarized calculations with Ce U_{4f} = 5 eV and J_{4f} = 0 eV. In fact, the lattice constants and band gap are little affected by the choice of the (U, J) parameter set of Gd, because the concentration of doped Gd is not sufficient to dominate those properties. Gd U_{4f} = 6.7 eV and J_{4f} = 0.7 eV are taken for further investigation because they are well optimized as demonstrated in previous work.[34] Some important parameters of the fully optimized structure are summarized in Table 2 to compare with experimental findings.

C. Y-codoped GDC

One of six Gds in $Ce_{26}Gd_6O_{61}$ is replaced by Y so that there are six structure configurations considered. The on-site coulomb interaction on the Y 4d orbitals is modeled by U = 3 eV and J = 0 eV.[35] The difference between the lowest and the highest total energy in the six configurations is 0.05 eV, with the structure in which the Y dopant has four next nearest Gd neighbours (nearest neighbor of Y is O) generates the highest total energy. This implies that the doping in experiments should be relatively uniform.

Using Bader analysis[36] we compare the charge of $Ce_{26}Gd_6O_{61}$ and Y-doped GDC. The O nns of Y gain more charge from Y than from Gd after substitution. However, the charge of Ce and other O atoms almost does not change. All the 6 configurations show this charge increase which is around 0.03 in the O sphere. The increase indicates that the ionic nature of the bonds is enhanced and, therefore, that the covalency and strength are reduced. The Gd–O and Y–O bond lengths are also inspected. If the Gd–O and Y–O bonds are of the same strength, Gd–O should be longer than Y–O because of a slightly larger radius of Gd. Nevertheless, the average Y–O bond length (2.465 Å) is larger than the average Gd–O bond length (2.461 Å), demonstrating that the Y–O bond is weaker than the Gd–O bond.

Partial densities of states (PDOSs) of GDC are depicted in Fig. 5. The electronic structures of the six configurations are similar. We therefore address only the one with the lowest total energy in Fig. 6. The same group of atoms in GDC and Y-doped GDC is taken to plot the PDOS of Gd (Y), one O nn and the Ce connected by this O. In Fig. 5, the O 2p PDOS shows hybridization with the Gd 5d states from −3.6 eV to −2.4 eV and both with the Gd 5d and Ce 4f states from −2.4 eV to 0 eV and 2.1 eV to 2.7 eV. A similar picture is obtained in Fig. 6 for the PDOS in Y-doped GDC. However, as the arrows shown in Fig. 5(b) and 6(b) highlight, the hybridization with the Y 4d states is obviously not as strong as that with the Gd 5d states. Furthermore, the O 2p contributions from 2.1 eV to 2.7 eV in Fig. 6 are more pronounced than in Fig 5. In fact, the increased hybridization between the Ce 4f and O 2p states is related to the decrease in the Y–O hybridization. We conclude that the Y–O bonds are weaker than the Gd–O bonds, which supports our findings from the Bader analysis and the bond lengths.

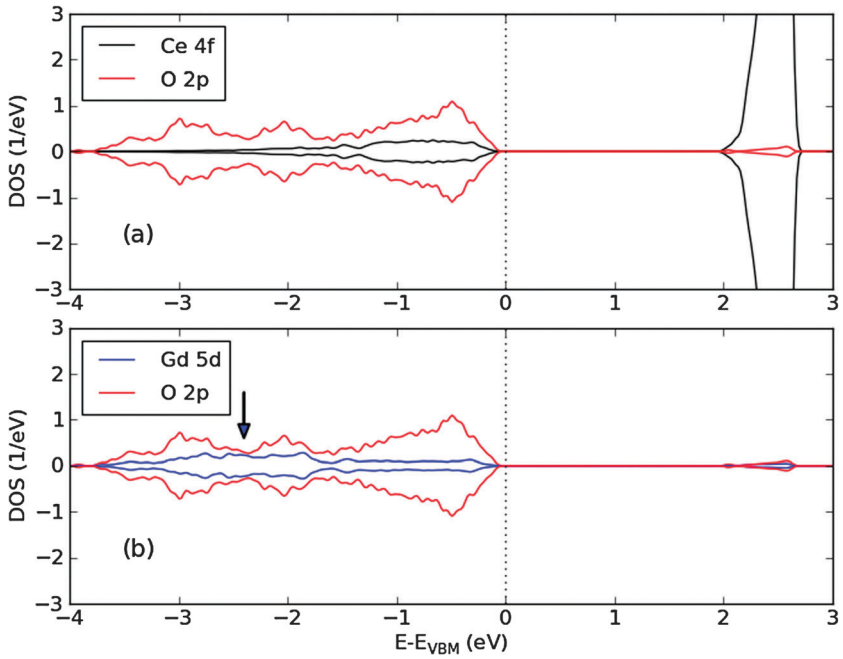

Fig. 5 PDOS of Ce 4f, Gd 5d, and O 2p in $Ce_{26}Gd_6O_{61}$. The arrow points at the difference between Gd–O and Y–O hybridization.

 This journal is © the Owner Societies 2012

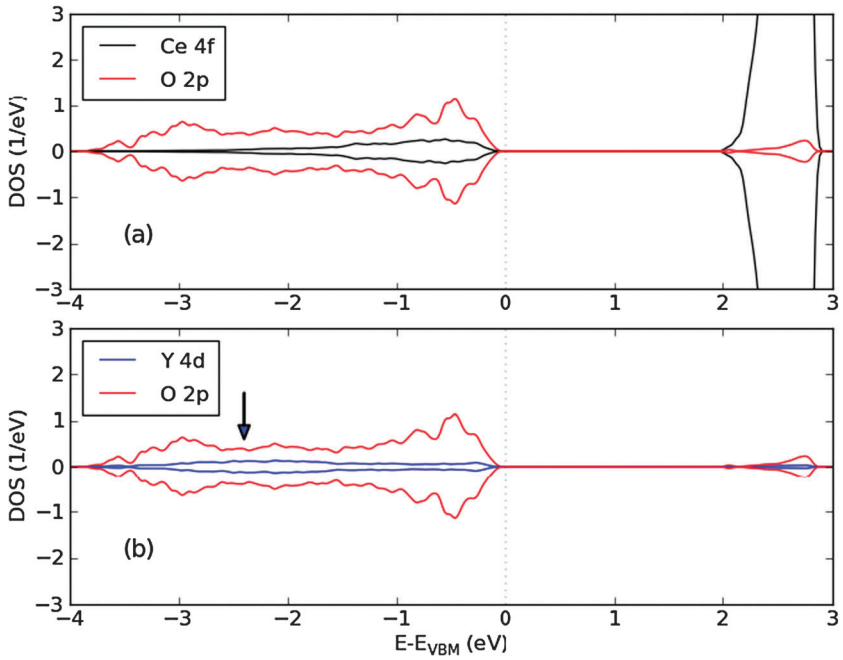

Fig. 6 PDOS of Ce 4f, Y 4d, and O 2p in the most energy favorable Y-doped $Ce_{26}Gd_6O_{61}$ structure. The arrow points at the difference between Gd–O and Y–O hybridization.

Published on 09 July 2012 on http://pubs.rsc.org | doi:10.1039/C2CP41202K
Downloaded by Open University on 20 October 2012

Conclusions

The present study aims to aid the community in unravelling the intricacies of defect processes in GDC and related materials such as YSZ using a computationally tractable methodology. In particular we propose two SQS cells to mimic the local pair correlation functions of GDC for two technologically important compositions. The use of these SQS structures will allow the implementation of DFT or other electronic structure calculations to investigate such systems in a realistic way. Importantly, as the SQS method is not a mean-field approach, the distribution of distinct local environments is preserved. The average of them corresponds to the random alloy. The results of our DFT calculations reveal that it is energetically favourable for the system when the Y is not close to other dopant atoms or oxygen vacancies. Our Bader analysis shows that O gains more charge from Y than from Gd, so that the covalent bond is weakened. The Y–O bond length is slightly longer than the Gd–O bond length and the obtained PDOSs illustrate that the Y 4d and O 2p hybridization is weaker than the Gd 5d and O 2p hybridization. These two findings demonstrate that the Y–O bonds are weaker than the Gd–O bonds. Hence, the substitution of Gd by Y in GDC is expected to improve the conductivity of O^{2-}. An enhancement of the ionic conductivity in Gd^{3+} and Y^{3+} codoped ceria as compared to singly Gd^{3+} or Y^{3+} doped ceria has been reported in ref. 37 and is fully in line with the picture derived from our calculations.

Acknowledgements

CJ acknowledges support by the National Natural Science Foundation of China (Grants No. 50901091 and 51071180).

References

1 N. P. Brandon, S. Skinner and B. C. H. Steele, *Annu. Rev. Mater. Res.*, 2003, **33**, 183.
2 J. Fleig, *Annu. Rev. Mater. Res.*, 2003, **33**, 361.
3 S. J. Skinner, *Int. J. Inorg. Mater.*, 2001, **3**, 113.
4 Z. Shao, S. M. Haile, J. Ahn, P. D. Ronney, Z. Zhan and S. A. Barnett, *Nature*, 2005, **435**, 795.
5 I. Seymour, A. Chroneos, J. A. Kilner and R. W. Grimes, *Phys. Chem. Chem. Phys.*, 2011, **13**, 15305; D. Rupasov, A. Chroneos, D. Parfitt, J. A. Kilner, R. W. Grimes, S. Ya. Istomin and E. V. Antipov, *Phys. Rev. B: Condens. Matter Mater. Phys.*, 2009, **79**, 172102; A. Chroneos, B. Yildiz, A. Tarancón, D. Parfitt and J. A. Kilner, *Energy Environ. Sci.*, 2011, **4**, 2774; I. D. Seymour, A. Tarancón, A. Chroneos, D. Parfitt, J. A. Kilner and R. W. Grimes, *Solid State Ionics*, 2012, **216**, 41.
6 A. Kushima, D. Parfitt, A. Chroneos, B. Yildiz, J. A. Kilner and R. W. Grimes, *Phys. Chem. Chem. Phys.*, 2011, **13**, 2242; D. Parfitt, A. Chroneos, A. Tarancón and J. A. Kilner, *J. Mater. Chem.*, 2011, **21**, 2183.
7 A. Chroneos, D. Parfitt, J. A. Kilner and R. W. Grimes, *J. Mater. Chem.*, 2010, **20**, 266.
8 D. Parfitt, A. Chroneos, J. A. Kilner and R. W. Grimes, *Phys. Chem. Chem. Phys.*, 2010, **12**, 6834.
9 N. Sata, K. Eberman, K. Eberl and J. Maier, *Nature*, 2000, **408**, 946.
10 T. Suzuki, I. Kosacki and H. U. Anderson, *Solid State Ionics*, 2002, **151**, 111.
11 I. Kosacki, C. M. Rouleau, P. F. Becher, J. Bentley and D. H. Lowndes, *Solid State Ionics*, 2005, **176**, 1319.
12 X. X. Guo, I. Matei, J. S. Lee and J. Maier, *Appl. Phys. Lett.*, 2007, **92**, 103102.
13 J. G. Barriocanal, A. R. Calzada, M. Varela, Z. Sefrioui, E. Iborra, C. Leon, S. J. Pennycook and J. Santamaria, *Science*, 2008, **321**, 676.
14 J. A. Kilner, *Nat. Mater.*, 2008, **7**, 838.
15 A. Kushima and B. Yildiz, *J. Mater. Chem.*, 2010, **20**, 4809.
16 X. Xie, R. V. Kumar, J. Sun and L. J. Henson, *J. Power Sources*, 2010, **195**, 5660.
17 A. Zunger, S. H. Wei, L. G. Ferreira and J. E. Bernard, *Phys. Rev. Lett.*, 1990, **65**, 353.
18 C. Jiang, C. Wolverton, J. Sofo, L. Q. Chen and Z. K. Liu, *Phys. Rev. B: Condens. Matter Mater. Phys.*, 2004, **69**, 214202.

View Online

19 A. Chroneos, C. Jiang, R. W. Grimes, U. Schwingenschlögl and H. Bracht, *Appl. Phys. Lett.*, 2009, **95**, 112101.
20 C. Jiang, C. R. Stanek, K. E. Sickafus and B. P. Uberuaga, *Phys. Rev. B: Condens. Matter Mater. Phys.*, 2009, **79**, 104203.
21 S. T. Murphy, A. Chroneos, C. Jiang, U. Schwingenschlögl and R. W. Grimes, *Phys. Rev. B: Condens. Matter Mater. Phys.*, 2010, **82**, 073201.
22 G. Kresse and D. Joubert, *Phys. Rev. B: Condens. Matter Mater. Phys.*, 1999, **59**, 1758.
23 J. P. Perdew, M. Ernzerhof and K. Burke, *J. Chem. Phys.*, 1996, **105**, 9982.
24 P. E. Blöchel, *Phys. Rev. B: Condens. Matter Mater. Phys.*, 1994, **50**, 17953.
25 S. Sameshima, H. Ono, K. Higashi, K. Sonoda, Y. Hirata and Y. Ikuma, *J. Ceram. Soc. Jpn.*, 2000, **108**, 1060.
26 A. I. Liechtenstein, V. I. Anisimov and J. Zaane, *Phys. Rev. B: Condens. Matter Mater. Phys.*, 1995, **52**, R5467.
27 G. R. Li, D. L. Qu, L. Arurault and Y. X. Tong, *J. Phys. Chem. C*, 2009, **113**, 1235–1241.
28 N. C. Hernandez, R. Grau-Crespo, N. H. de Leeuw and J. F. Sanz, *Phys. Chem. Chem. Phys.*, 2009, **11**, 5246.
29 A. Ismail, J. Hooper, J. B. Giorgi and T. K. Woo, *Phys. Chem. Chem. Phys.*, 2011, **13**, 6116.
30 V. I. Anisimov and O. Gunnarsson, *Phys. Rev. B: Condens. Matter Mater. Phys.*, 1991, **43**, 7570.
31 B. N. Harmon, V. P. Antropov, A. I. Liechtenstein, I. V. Solovyev and V. I. Anisimov, *J. Phys. Chem. Solids*, 1995, **56**, 1521.
32 M. Burbano, D. Marrocchelli, B. Yildiz, H. L. Tuller, S. T. Norberg, S. Hull, P. A. Madden and G. W. Watson, *J. Phys.: Condens. Matter*, 2011, **23**, 255402.
33 R. K. Singha, P. Kumari, A. Samariya, S. Kumar, S. C. Sharma, Y. T. Xing and E. B. Saitovitch, *Appl. Phys. Lett.*, 2010, **97**, 172503.
34 M. Petersen, J. Hafner and M. Marsman, *J. Phys.: Condens. Matter*, 2006, **18**, 7021.
35 B. Saha, T. D. Sands and U. V. Waghmare, *J. Appl. Phys.*, 2011, **109**, 073720.
36 W. Tang, E. Sanville and G. Henkelman, *J. Phys.: Condens. Matter*, 2009, **21**, 084204; E. Sanville, S. D. Kenny, R. Smith and G. Henkelman, *J. Comput. Chem.*, 2007, **28**, 899; G. Henkelman, A. Arnaldsson and H. Jónsson, *Comput. Mater. Sci.*, 2006, **36**, 254.
37 X. Guan, H. Zhou, Z. Liu, Y. Wang and J. Zhang, *Mater. Res. Bull.*, 2008, **43**, 1046.

Published on 09 July 2012 on http://pubs.rsc.org | doi:10.1039/C2CP41202K
Downloaded by Open University on 20 October 2012

 This journal is © the Owner Societies 2012